8 July 1983, Volume 221, Number 4606 SCIENCE

Microfabrication as a Scientific Tool

R. E. Howard, P. F. Liao, W. J. Skocpol
L. D. Jackel, H. G. Craighead

Summary. Research in microfabrication not only serves the microelectronics industry but also can provide research tools for studying the behavior of matter at submicrometer dimensions. A variety of techniques including optical, x-ray, and electron beam lithography and reactive ion etching can be used to make structures, devices, and arrays only hundreds of atoms across. Microfabrication techniques have been applied to experiments on surface-enhanced Raman scattering, transport in one-dimensional conductors, and macroscopic quantum tunneling. Recent progress is extending these techniques to scales of less than 100 angstroms.

Before the invention of printing, books had to be made by drawing each character by hand. Now, modern lithographic techniques can directly reproduce whole pages containing both characters and high-resolution photographs. Similarly, electronic components, once made one at a time, can now be made extraordinarily small and simultaneously fabricated by the millions. The techniques required include highly refined versions of lithographic processes like those used in the graphic arts trade, and special processes such as ion implantation that are unique to solid-state electronics. High-speed printing processes made books universal commodities; microfabrication is having a similar effect on semiconductor devices.

But research in microfabrication does more than serve the microelectronics industry. When size scales can be measured in hundreds of atoms, new areas of science beg to be explored. In this article, we introduce processes used for microfabrication and give examples of their application to fundamental research.

The authors are members of the technical staff of Bell Laboratories, Holmdel, New Jersey 07733.

Microfabrication

Pattern generation is usually done with a lithographic technique, shown schematically in Fig. 1 (*1*). A substrate to be patterned is coated with a radiation-sensitive material (usually a polymer) whose solubility in a developer is a function of irradiation. After development, the resist has a relief profile, as shown in Fig. 1, that can be used to transfer the pattern to the substrate. This resist pattern can be used as a mask for etching the substrate, or as a stencil for selective deposition of a film on the substrate.

In most commercial integrated circuit manufacture, optical lithography is used to transfer a mask pattern into the resist layer. The process is fast and inexpensive, but the resolution is limited by diffraction to dimensions a few times the wavelength of light, about 1 μm. This limit can be extended by using shorter wavelength photons (x-rays); x-ray lithography (*2*) has reproduced patterns with dimensions as small as 175 Å.

Some specialized submicrometer patterns can be created and exposed directly by the interference of laser beams (holography) (*3*). These can be used, for example, to make zone plates (*4*) or arrays of small particles (*5*). Primary generation of high-resolution patterns is usually done, however, by using a focused beam of electrons to write directly on a resist layer. This method has the highest demonstrated resolution of any lithographic technique. The main resolution limitation on electron beam lithography is diffuse exposure from electrons scattered by the resist and the substrate, although patterns as fine as 20 Å have been formed on thin (< 1000 Å) membrane substrates, where electron scattering effects on the exposure are negligible (*6*). On thick substrates, where the scattering effects are more limiting but the experiments more interesting, techniques have been developed to make patterns as fine as 100 Å (*7*) and to make electronic devices with minimum features well under 1000 Å (*8, 9*). This opens to study a new size regime of transport phenomena. In later sections we will describe some of the experiments made possible by these developments and indicate progress toward even higher resolution fabrication.

Light Scattering in Submicrometer Arrays

When light is scattered by molecules, a very small fraction of the light is found to have a frequency, and therefore a wavelength, which differs from that of the incident light. The shift in frequency is precisely equal to the frequency of a molecular vibration. Because vibrational frequencies are characteristic of molecular species, the spectrum of the scattered light (Raman spectrum) is useful for the study of molecular interactions and processes.

Recently, experimental physicists and chemists studying laser-induced Raman spectra of molecules discovered that molecules adsorbed on suitably roughened silver surfaces produced unusually large signals (*10*); the intensity of the Raman spectrum can be increased by factors of 10^4 to 10^7 on such surfaces. This increase allows easy detection of a submonolayer coverage of molecules on a surface and presents the opportunity to obtain detailed information about mole-

cules on surfaces by means of Raman spectroscopy. Furthermore, such roughened surfaces enhance many other optical processes such as second harmonic generation (*11*), dye luminescence (*12*), two-photon absorption (*13*), and tunnel diode detector response (*14*). The mechanism of the enhancement is quite controversial, however, and many experiments have been performed to investigate it.

Because the typical size scale of the irregular roughness on surfaces that produce the largest enhancement is ~100 to 1000 Å, microfabrication techniques provide ideal tools for studying the phenomena. Recently, a collaborative effort between Bell Laboratories and the Massachusetts Institute of Technology led to the development of a lithographic fabrication technique (*5*) that avoids chemical contamination of the silver and yet generates uniformly textured surfaces. The new technique produces an array of uniform silver ellipsoids by evaporating silver at grazing incidence onto a patterned SiO_2 substrate. The pattern is made by using laser holography to expose photoresist, followed by reactive ion etching (etching of the substrate by ion bombardment in a halogen-containing plasma) to produce a square array of 5000-Å-tall SiO_2 posts having diameters of 1000 Å and separated by 3000 Å (Fig. 2). After evaporation of the silver, the top of each post supports an identical silver particle. Particle arrays of other metals can be obtained in the same manner. These arrays of particles allow detailed tests of the "electromagnetic theory" of enhanced Raman scattering.

The electromagnetic theory, proposed by Moskovits (*15*) and elaborated on by several groups (*16*), attributes much of the total Raman enhancement to the plasmon resonance of a silver particle. (A plasmon is a density oscillation of electrons in a metal.) The plasmon resonance frequency is determined by the shape and dielectric properties of the metal particle. The interaction of the incident laser field with this resonance results in a large local field at the surface of the particle, inducing a large Raman polarization in any adsorbed molecules. The outgoing Raman radiation is also enhanced as the molecular fields polarize the resonant particles, producing large oscillating dipole moments. Indeed, the particle dipole moments are so large that the total enhancement is eventually limited by the loss of energy through radiation, that is, radiation damping (*17*).

Figure 3 shows the enhancement of the Raman spectrum of CN molecules adsorbed on silver and on gold particle arrays (*18*). The line drawn through the data for silver particles is a fit to the electromagnetic theory for the plasmon resonances of ellipsoidal particles, using the dielectric constants of silver and including radiation damping. Only the particle dimensions were treated as adjustable. The fit implied dimensions of 2000 by 550 Å, in fair agreement with the measured particle dimensions. Using the same dimensions, one can predict the enhancement by gold particles of the same shape, and this prediction is shown in Fig. 3 as the dashed line. The close agreement between experiment and theoretical prediction verifies the importance of electromagnetic effects and demonstrates the power of microfabrication to help unravel the physics of peculiar phenomena associated with matter of small dimensions.

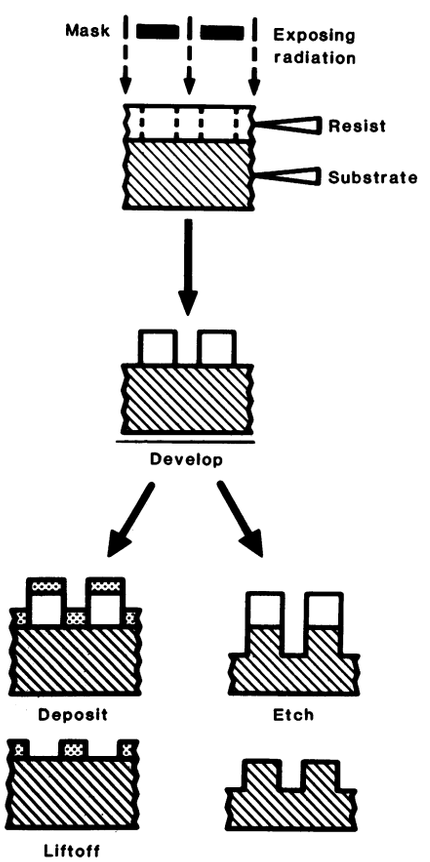

Fig. 1 (left). Schematic of the lithographic process. A development process forms a pattern in a resist layer after exposure by a suitable radiation (light, x-rays, electrons, or ions). This pattern can then be used as a stencil for subsequent patterning of either the substrate or a deposited film. Fig. 2 (right). Electron micrograph of a patterned SiO_2 substrate used in studies of enhanced Raman scattering. The calibration bar is 1000 Å long.

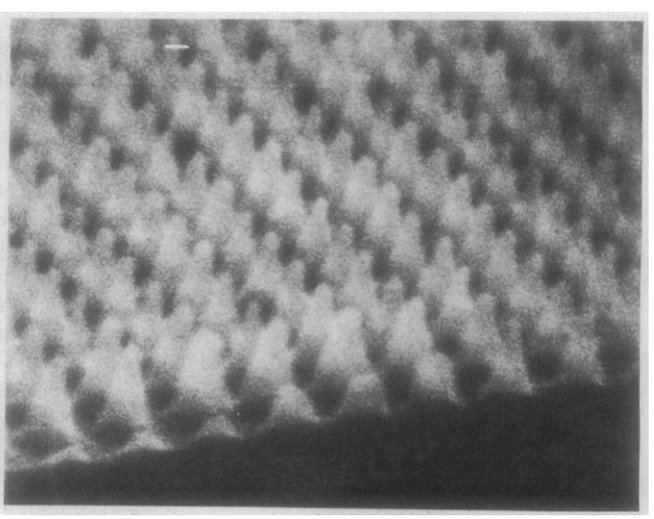

Transport in Restricted Geometries

The conductivity of metals ordinarily increases as the temperature is lowered. This ceases to be true in extremely disordered materials, because at low temperatures the electrons become trapped in localized states and their Coulomb interaction effects are modified (*19*). Even weakly disordered metals can show similar nonmetallic effects if they are small in one or more dimensions, altering the diffusion of electrons. This has been observed below 1 K in thin metal films (*20*) and at even higher temperatures in narrow metal wires (*21*). (The latter can be made as small as 200 Å by various combinations of etching and oblique evaporation.) However, the fractional conductivity changes are small ($<< 0.1$ percent) because the electron density is large and unadjustable.

The same effects can be studied more comprehensively in semiconductor device structures which contain thin electrically controllable layers of electrons at metallic densities. In a metal-oxide-semiconductor field-effect transistor (MOSFET) such a layer is formed in order to control the conduction between the source and drain contacts (electron-rich *n*-type regions implanted at the surface of the *p*-type semiconductor). The channel region between the source and the drain is depleted of holes and forms a thin layer of electrons when a sufficiently large positive voltage is applied to the

metal gate. (The gate is located above the channel but isolated from it by oxide. The sandwich structure forms a parallel plate capacitor, in which the positive charge on the gate must be matched by a layer of negative charge at the oxide-semiconductor interface.) Once the applied voltage exceeds the threshold required for formation of an electron layer, the density of the layer will be directly proportional to the excess gate voltage. Like metal films, these inversion layers show decreases of conductance at low temperatures, but they can be more easily controlled and characterized, allowing definitive comparisons with theory (*22*).

Narrow inversion channels are analogous to narrow metal wires, and we have made channels as narrow as 1000 Å by using electron beam lithography and reactive ion etching. High-resolution lithography (*23*) and liftoff are used to pattern a parallel array of very narrow metal gates. These in turn serve as self-aligning masks that protect narrow channels during reactive ion etching (through the unprotected oxide and into the silicon substrate). Figure 4 shows the resulting structure of parallel narrow (1000 Å) pedestals which confine the electron inversion layers at the oxide-silicon interface to the same width as the gate (*24*). Our experiment involves measuring the conductance from source to drain of these channels at low temperatures.

Figure 5 shows channel conductance as a function of temperature for a number of different gate voltages above threshold, corresponding to different electron densities. At each fixed density, the conductance decreases at low temperatures, showing strongly nonmetallic behavior. Starting from the observed value of conductance at 30 K, each dotted curve represents the nonmetallic change of conductance predicted by the one-dimensional versions of the combined localization and interaction theories (*25, 26*), using only parameters determined from two-dimensional inversion layers and the known geometry of the narrow channels. The one-dimensional theory is appropriate, because each channel is narrower than the electron diffusion lengths identified by the theory. The effect is quantum mechanical in nature, because its magnitude is proportional to the conductance unit e^2/h, where e is the electronic charge and h is Planck's constant.

In the experiment above, we placed many channels in parallel in order to measure the conductance in a convenient range. The resulting averaging tended also to cause the conductance to

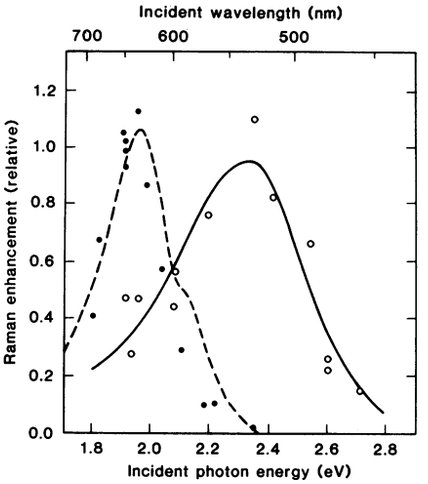

Fig. 3. Excitation photon energy dependence of Raman enhancement for (○) silver and (●) gold particles supported on patterned SiO_2 substrates. The solid line is a fit to the electromagnetic theory for the silver particle data and the dashed line is a fit to the data for the gold particles.

increase smoothly with gate voltage as electrons sequentially filled the various energy levels of the inversion layer (as required by the Pauli exclusion principle). In simpler devices with single short narrow gates, however, we find that the low-temperature conductivity actually has noticeable structure as a function of gate voltage. The patterns can be quite regular and are tantalizingly similar to the pattern of energy level spacings predicted for the quantized states of a "particle in a box" associated with the lithographically defined width. Workers at Yale (*27*) noted similar behavior in less narrow, but less disordered, submicrometer MOSFET's fabricated by optical lithography. The spacing of energy levels may affect the conductivity directly or through the interaction and localization effects. In any case, convincing evidence of this quantization of transverse motion in a narrow box—a standard example in introductory quantum mechanics textbooks—may soon be forthcoming. If so, it will be the first time the one-dimensional situation of motion quantized in two transverse directions has been demonstrated. (Even wide inversion layers are already fully quantized in the direction prependicular to the oxide-silicon interface because the inversion layer is only about 100 Å thick.)

Macroscopic Quantum Tunneling

A superconducting metal is another example of a system in which quantum mechanical effects can be important at size scales accessible by microfabrication techniques. When two superconducting films are separated by a thin, insulating oxide, a Josephson tunnel junction is formed. For oxides a few nanometers thick, superconducting electrons can tunnel through the oxide, causing a zero-voltage current to flow from one film to the other. The maximum supercurrent that can flow through the junction is called the critical current. When the current through a Josephson junction is increased, switching from the zero-voltage state to a finite-voltage state occurs randomly over a range of currents just less than theoretical critical current.

For most junctions this distribution is due to thermal fluctuations (*28*). In the zero-voltage state the system is constrained by an energy barrier to remain in a potential well. As the applied current is increased, the energy barrier separating the zero-voltage and finite-voltage states is reduced; this barrier becomes zero at the critical current and the system must switch to the finite-voltage state. However, for current slightly below the critical current, the barrier is

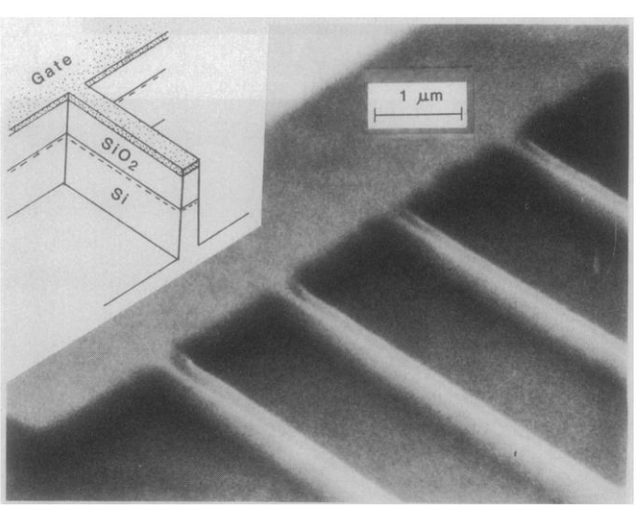

Fig. 4. Perspective view of MOSFET structure with narrow conducting channels for studying one-dimensional transport. An electron inversion layer forms at the Si-SiO_2 interface and completes the circuit between source and drain contacts (not shown).

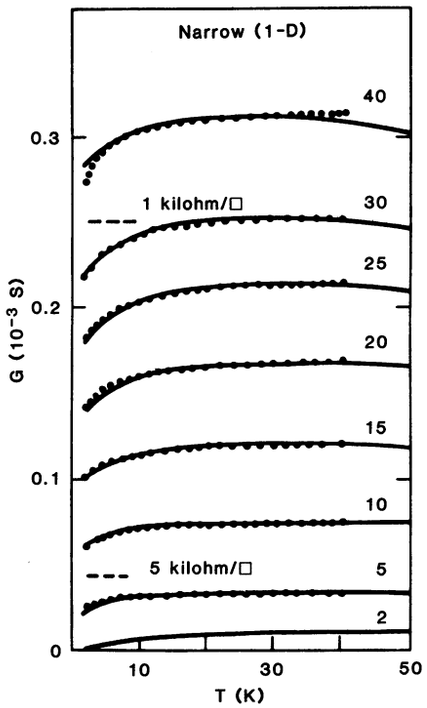

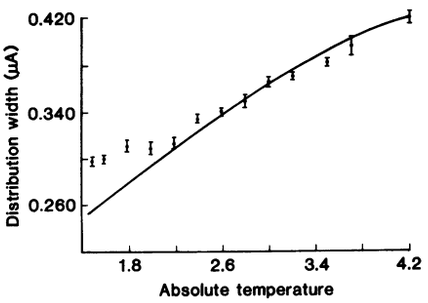

Fig. 5 (left). Channel conductance as a function of temperature with gate voltage above threshold as a label. Solid curves are experimental data, showing strong nonmetallic conductance decreases at low temperatures. Dotted curves are the changes predicted by one-dimensional theory. Fig. 6 (right). Distribution width of measured critical currents in a small Josephson tunnel junction as a function of temperature. The solid line represents the thermal theory for our data. The departure of the data from this line below 2.2 K is attributed to the effects of macroscopic quantum tunneling.

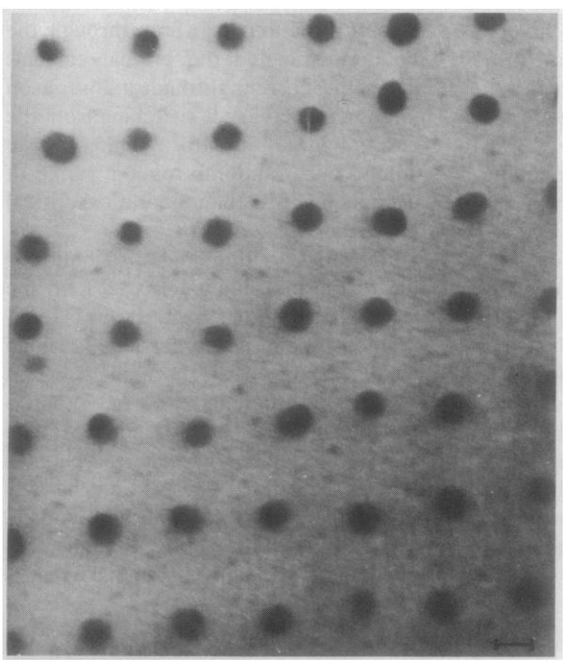

Fig. 7. Array of gold-palladium dots on a carbon membrane. The size of the calibration mark is 100 Å.

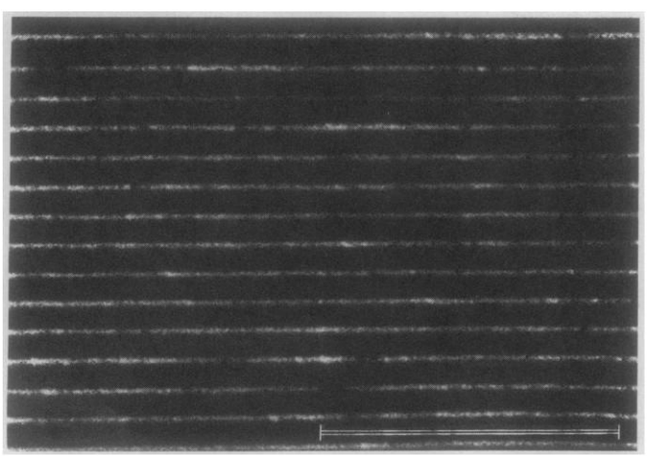

Fig. 8. Gold-palladium lines 100 Å wide on a thick silicon substrate made with high-voltage electron beam lithography.

small, and thermal fluctuations can drive the system over the barrier to the finite-voltage state. As temperature, T, is reduced, the thermal fluctuation effects are reduced and the transitions occur over a narrower range closer to the critical current.

The transition width does not go to zero as T nears zero, however, because quantum mechanical tunneling provides another mechanism for barrier escape. Under the right conditions, systems can tunnel through an energy barrier without the help of thermal activation. In such a system, the thickness of the barrier scales with the width of the potential well; simple arguments suggest that tunnel escape should dominate over thermal escape when the energy spacings in the well are larger than the available thermal energy. However, recent theoretical work (*29*) has shown that resistive damping in the junction reduces tunneling escape so that it is only observed at much lower temperatures.

In a Josephson junction, the energy spacings are given by Planck's constant times the electromagnetic resonance frequency of the junction, which is proportional to the square root of the junction capacitance. For most Josephson junctions, both the capacitance and the resistive damping are so large that tunneling is expected to be important only below one-hundredth of a degree, a temperature difficult to achieve experimentally. However, we have made junctions sufficiently small that low capacitance (a few femtofarads) allows tunnel escape to be observed at 2 K (*30*) (see Fig. 6).

The simplicity of Josephson junctions makes them prime candidates for miniaturization. By sequential evaporation at various angles through a suspended resist stencil (*31*), Josephson edge-junctions (*32*) can be formed in which the thickness of one film determines one dimension of the junction area. Thus, by using optical lithography it is possible to make junctions with dimensions of 1 by 0.05 μm, small enough to see the effects shown in Fig. 6. Even smaller junctions can be made by applying this method to stencils drawn by electron beam lithography. Josephson junctions only 1000 Å on a side have been made with this technique (*8*); these are arguably the smallest electronic devices made in any technology.

We emphasize that this tunneling is not tunneling of a particle through a real space barrier, as in the case of the superconducting electrons tunneling through the oxide barrier. Instead, the phase difference (between the wave functions of the superconducting electrons on either side of the junction) tunnels through

a range of phase values with forbidden energy. Because the phase of the wave functions is nearly uniform throughout each superconducting film, this tunneling involves a large system and has thus been called macroscopic quantum tunneling (MQT). So far, the only systems to exhibit MQT have been ultrasmall Josephson junctions (*30, 33*).

Extending the Limits

The experiments discussed above have all been at the 1000-Å size scale or larger. With modified techniques it is possible to make structures at least an order of magnitude smaller; these may eventually be useful for studying additional quantum mechanical effects, ballistic electron transport, or even shape-sensitive catalysts.

The smallest lithographically defined structures have been made on thin-film substrates. Scanning transmission electron microscopes can produce focused electron beams with diameters as small as 2 Å and have been used directly to drill 20-Å holes in thin salt crystals (*6*). Another approach with thin films involves contamination lithography (*34*), in which carbonaceous deposits are formed on the surface wherever the electron beam decomposes adsorbed hydrocarbons. Material unprotected by the carbon can be removed by ion milling (*35, 36*). One example is shown in Fig. 7, a transmission electron micrograph of an array of gold-palladium alloy particles 50 Å in radius on an amorphous carbon supporting film ~100 Å thick (*36*). This figure shows a section of a larger square array of nearly uniform particles. There are only several thousand atoms in each particle.

This regular array of simple geometry is an ideal experimental system, sufficiently well characterized to test theoretical predictions of the electromagnetic response of inhomogeneous matter (*37*), such as the resonance Raman scattering described in an earlier section. In addition, at dimensions of ~100 Å quantum size effects should become observable (*38*), and some experiments have been performed on random arrays of particles with these dimensions (*39*). The structures in Fig. 7 are well within the size regime at which these new effects are expected.

While the techniques on thin substrates represent the ultimate in small-scale fabrication, progress is also being made in the fabrication of more versatile and sturdy samples on thick substrates of the kind used for semiconductor devices.

We recently showed that the limits of "conventional" electron beam lithography can be extended to the 100-Å range (*7*), more than a factor of 2 smaller than previously possible. Figure 8 shows a scanning electron micrograph of 100-Å-wide metal lines with 400-Å spaces formed on a piece of a silicon wafer. This was done by exposing a thin (300 Å) layer of standard electron beam resist with an electron beam ~20 Å in diameter at an energy of 120 keV. The "wires" were formed by developing the exposed pattern, evaporating a gold-palladium alloy film, and lifting off the unwanted material. The small beam size and high beam energy combine to reduce the effects of backscattered electrons, which have limited previous work on this scale. Similar results have been obtained on GaAs, which, because its higher average atomic number increases electron backscattering, is more difficult than silicon to use as a substrate for high-resolution patterning (*7*).

The metal wires shown in Fig. 8 are 10 μm long but only about 100 atoms wide. Applications for these patterns include further investigations of the nonmetallic conductance at low temperatures and as gates for strictly one-dimensional MOSFET's. Other new effects, such as ballistic electron transport, may become observable in other structures smaller than the electron mean free path. With the discreteness of energy levels not only measurable but controllable, new types of electronic devices may be possible.

Finally, the scientific applications will certainly not be restricted to electronics. For example, many structure-sensitive catalysts depend on shapes with dimensions of 50 to 100 Å and construction possibilities at this size scale present exciting prospects.

Conclusions

New fabrication techniques are being developed that permit structures to be made with dimensions measured in hundreds of atoms or less. At these dimensions, quantum mechanical phenomena become important and a variety of new effects are being observed in such properties as electron transport and optical resonances. The expanding study of these effects is answering fundamental questions about the behavior of matter at submicrometer dimensions.

References and Notes

1. R. E. Howard and D. E. Prober, in *VLSI Electronics*, N. Einspruch, Ed. (Academic Press, New York, 1982), vol. 5
2. D. C. Flanders, *Appl. Phys. Lett.* **36**, 93 (1980).
3. H. I. Smith, *Proc. IEEE* **52**, 1361 (1964).
4. B. Niemann, D. Rudolph, G. Schmahl, *Opt. Commun.* **12**, 160 (1974).
5. P. F. Liao *et al.*, *Chem. Phys. Lett.* **82**, 355 (1981).
6. M. Isaacson and A. Murray, *J. Vac. Sci. Technol.* **19**, 1117 (1981).
7. H. G. Craighead, R. E. Howard, L. D. Jackel, P. M. Mankiewich, *Appl. Phys. Lett.* **42**, 38 (1983).
8. E. L. Hu, R. E. Howard, L. D. Jackel, L. A. Fetter, D. M. Tennant, *IEEE Trans. Electron Devices* **ED-27**, 2030 (1980).
9. R. E. Howard *et al.*, *IEEE Electron Device Lett.* **EDL-3**, 322 (1982); R. G. Swartz *et al.*, *1982 International Electron Devices Meeting Technical Digest* (IEEE, New York, 1982), p. 642.
10. M. Fleischman, P. J. Hendra, A. J. McQuillan, *Chem. Phys. Lett.* **26**, 163 (1974); for a recent review, see R. K. Chang and T. E. Furtak, Eds., *Surface Enhanced Raman Scattering* (Plenum, New York, 1982).
11. C. K. Chen, A. R. B. DeCastro, Y. R. Shen, *Phys. Rev. Lett.* **46**, 145 (1981); A. Wokaun, J. G. Bergman, J. P. Heritage, A. M. Glass, P. F. Liao, D. H. Olson, *Phys. Rev. B* **24**, 849 (1981).
12. A. M. Glass, P. F. Liao, J. G. Bergman, D. H. Olson, *Opt. Lett.* **5**, 368 (1980).
13. A. M. Glass, A. Wokaun, J. P. Heritage, J. G. Bergman, P. F. Liao, D. H. Olson, *Phys. Rev. B* **24**, 4906 (1981).
14. A. M. Glass, P. F. Liao, D. H. Olson, L. M. Humphrey, *Opt. Lett.* **7**, 575 (1982).
15. M. Moskovits, *J. Chem. Phys.* **69**, 4159 (1978).
16. S. L. McCall, P. M. Platzman, P. A. Wolff, *Phys. Lett. A* **77**, 381 (1980); M. Kerker, D. S. Wang, H. Chen, *Appl. Opt.* **19**, 4159 (1980); C. Y. Chen and E. Burstein, *Phys. Rev. Lett.* **45**, 1287 (1980); J. I. Gersten and A. Nitzan, *J. Chem. Phys.* **73**, 3023 (1980).
17. A. Wokaun, J. P. Gordon, P. F. Liao, *Phys. Rev. Lett.* **48**, 957 (1982).
18. P. F. Liao and M. Stern, *Opt. Lett.* **7**, 483 (1982).
19. For a recent review see G. A. Thomas, *Physica (Amsterdam)* **117B-118B**, 81 (1983); G. A. Thomas *et al.*, *Phys. Rev. B* **26**, 2113 (1982).
20. G. J. Dolan and D. D. Osheroff, *Phys. Rev. Lett.* **43**, 721 (1979); for a recent review, see G. Deutscher and H. Fukuyama, *Phys. Rev. B* **25**, 4298 (1982).
21. N. Giordano, W. Gilson, D. E. Prober, *Phys. Rev. Lett.* **43**, 725 (1979); for a recent review, see A. E. White, M. Tinkham, W. J. Skocpol, D. C. Flanders, *ibid.* **48**, 1752 (1982).
22. For example, D. J. Bishop, D. C. Tsui, R. C. Dynes, *ibid.* **44**, 1153 (1980); *Phys. Rev. B* **26**, 773 (1982).
23. R. E. Howard, E. L. Hu, L. D. Jackel, *IEEE Trans. Electron Devices* **ED-28**, 1378 (1981).
24. W. J. Skocpol, L. D. Jackel, E. L. Hu, R. E. Howard, L. A. Fetter, *Phys. Rev. Lett.* **49**, 951 (1982).
25. D. J. Thouless, *Solid State Commun.* **34**, 683 (1980).
26. B. L. Altshuler, D. Khmel'nitzkii, A. I. Larkin, P. A. Lee, *Phys. Rev. B* **22**, 5142 (1980).
27. R. G. Wheeler, private communication.
28. T. A. Fulton and L. N. Dunkleberger, *Phys. Rev. B* **9**, 4760 (1974).
29. A. O. Caldeira and A. J. Leggett, *Phys. Rev. Lett.* **46**, 211 (1981).
30. L. D. Jackel *et al.*, *Bull. Am. Phys. Soc.* **26**, 382 (1981); *Phys. Rev. Lett.* **47**, 697 (1981).
31. G. J. Dolan, *Appl. Phys. Lett.* **31**, 337 (1977).
32. M. Heiblum, S. Wang, J. R. Whinnery, T. K. Gustafson, *IEEE J. Quantum Electron.* **QE-14**, 159 (1978); R. H. Havemann, *J. Vac. Sci. Technol.* **15**, 389 (1978); R. E. Howard, E. L. Hu, L. D. Jackel, L. A. Fetter, R. H. Bosworth, *Appl. Phys. Lett* **35**, 879 (1979).
33. R. F. Voss and R. A. Webb, *Phys. Rev. Lett.* **47**, 265 (1981).
34. A. N. Broers, W. W. Molzen, J. J. Cuomo, N. D. Wittels, *Appl. Phys. Lett.* **29**, 596 (1976).
35. R. B. Laibowitz, A. N. Broers, J. T. C. Yeh, J. M. Viggiano, *ibid.* **37**, 891 (1979).
36. H. G. Craighead and P. M. Mankiewich, *J. Appl. Phys.* **53**, 7186 (1982).
37. W. Lamb, D. M. Wood, N. W. Ashcroft, *Phys. Rev. B* **21**, 2448 (1980).
38. M. Cini, *J. Opt. Soc. Am.* **71**, 386 (1981).
39. L. Genzel, T. P. Martin, U. Kreibig, *Z. Phys. B* **21**, 339 (1975); U. Kreibig, *ibid.* **31**, 39 (1978).